energies

MDPI

Article

Quantitative Research of Photobioreactor Performance Based on an Improved Surface Fitting Method

Qihang Jin, Zhenzong He * and Huijie Ma

Jiangsu Province Key Laboratory of Aerospace Power System, College of Energy and Power Engineering, Nanjing University of Aeronautics and Astronautics, Nanjing 210016, China; qihangjin1998@gmail.com (Q.J.); jeusma17@gmail.com (H.M.)

* Correspondence: hezhenzong@nuaa.edu.cn; Tel.: +86-187-6165-4116

Received: 31 August 2019; Accepted: 23 October 2019; Published: 26 October 2019

Abstract: The relationship between performance and working conditions in photobioreactor hydrogen production systems illuminated by a variable intensity light source has been described quantitatively using relational expressions. First, based on the finite volume method and the Michaelis-Menten model, the hydrogen production process of a photobioreactor (PBR) system was simulated numerically. Then, the performance of the PBR system was evaluated considering the hydrogen production rate, dimensionless hydrogen production rate, hydrogen production thrust coefficient and conversion efficiency of light energy to hydrogen energy rate as performance parameters, and the relationship between these parameters and working conditions was studied. Finally, the improved quantum-behaved particle swarm optimization (IQPSO) and surface fitting technique based on the curve fitting method were used to obtain relational expressions about the performance and working conditions of the PBR. All of the results show that the method can obtain accurately relational expressions for the performance optimization and forecasts of the PBR system.

Keywords: microalgae photobiological H_2 production; light transfer; photobioreactor; fitting of curve and surface

1. Introduction

With the development of the economy and improvements in quality of life, the demand for energy is increasing. Meanwhile, the exploitation and utilization of irreproducible fossil fuels worldwide has made energy crises, environmental pollution, and global warming increasingly prominent. Thus, there is an urgent need to seek a renewable and clean energy source as an alternative. To date, hydrogen energy has been regarded as an ideal alternative energy source because of the clean byproduct (i.e., water vapor) produced from its reaction with oxygen and the varieties of production methods [1–3]. Among the various production methods, the photobiological hydrogen production of microorganisms is considered to be an important potential method, since hydrogen production processes are operated at ambient temperatures and pressures.

The photobiological hydrogen production processes of microorganisms can be classified as follows:

1. Photolysis of water using algae and cyanobacteria [4]. For green algae, the electrons are derived from water under the light and used to reduce protons, to produce a hydrogen molecule with hydrogenase enzymes in a hydrogen production process. However, for cyanobacteria and blue-green algae, the electrons from the photolysis process of water are first converted into organic molecules. Then, these organic molecules are degraded and the electrons are used by the hydrogenase and/or nitrogenase enzymes to produce hydrogen.

2. Photodecomposition of organic compounds by photosynthetic bacteria [4]. For hydrogen production of photosynthetic bacteria, the electrons are derived from external organic medium of photosynthetic bacteria in photo-fermentation and are used by nitrogenase to generate H_2.

In the processes of photobiological hydrogen production of cyanobacteria, levels of around 30% O_2 in the mixed gases with H_2 is dangerous for the system. In addition, the processes of hydrogen production of photosynthetic bacteria cause water pollution and CO_2 emissions [4]. In photobiological H_2 production system of green algae, hydrogenase is particularly sensitive to O_2 [5]. Melis et al. [6,7] showed that pure hydrogen production can be achieved by Chlamydomonas reinhardtii under sulfur deprivation. This means that the oxygen inhibition of hydrogenase and the danger of gases mixed with H_2 and O_2 can be avoided. In fact, the photobiological H_2 production process of C. reinhardtii can generally be divided into three phases. In the first phase, C. reinhardtii grows through ordinary photosynthesis. In the second phase, C. reinhardtii is cultured in a sulfur-deprived medium, and O_2 production is slowed down. In the third phase, the anaerobic state of cells is achieved by sulfur deprivation, and cells produce pure hydrogen. Until now, the Chlamydomonas reinhardtii has been regarded as a potential best candidate for photobiological hydrogen production, because of its abilities to absorb CO_2 and large photosynthetic efficiency, which are larger than higher plants (e.g., tree or sugar cane) [8]. Moreover, the hydrogen production of C. reinhardtii has been studied extensively [9], and this means that mass data experimental data, radiation characteristics and characteristic parameters of the photobiological H_2 production model can be used as a reference. Therefore, the investigation of C. reinhardtii CC125, commonly used in H_2 production, was chosen to theoretically study the photobiological hydrogen production process of the photobioreactors in the present work.

Photobioreactors (PBR) are enclosures used to cultivate microorganisms that utilize light as their energy source for their growth and subsequent product formation [10]. Recently, numerous numerical simulations of the H_2 production process in the PBR have been studied extensively for optimizing the design, operation, and performance of the PBRs. Aiba [11] simulated the distribution and absorptance of light intensity of a one-dimensional plane-parallel photobioreactor with microalgae Rhodopseudomonas spheroides. Berberoglu and Pilon [12] investigated the effect of a mixed culture with C. reinhardtii CC125 and R. sphearoides ATCC 49419 on the conversion efficiency of solar energy to hydrogen energy and hydrogen productivity in plane-parallel PBR. Murphy and Berberoglu [13] calculated the productivity of a C. reinhardtii wild strain and transformant tla1 in plane-parallel PBRs coupling the light transfer model with photosynthetic rate model. In addition, the local specific and total oxygen production as a function of optical thickness at different incident irradiances was calculated in plane-parallel PBRs. Wheaton and Krishnamoorthy [14] simulated light transfer coupled with fluid hydrodynamics in an air-lift tubular photobioreactor illuminated from inside by fluorescent lamps. Slegers et al. [15] simulated outdoor vertical flat-plate PBRs containing Phaeodactylum tricornutum or Thalassiosira pseudonana of continuous culture. Moreover, the effect of PBR thickness and biomass concentration on the volumetric productivity has been studied. Pruvost et al. [16] simulated outdoor inclined rectangular PBR illuminated by solar irradiance with cyanobacterium Arthrospira platensis of continuous cultivation, and the calculation of the areal biomass productivity per unit surface area is based on light transfer model and growth kinetics model. Lee et al. [17] demonstrated that it is necessary to optimize light intensity, cell density, and the optical thickness of the PBR for maximizing microalgal productivity for a given microalgae species in the process of design and operation of PBR. Moreover, they obtained qualitative guidelines from experimental studies. Zhang et al. [18] investigated the effect of solar irradiation, microalgae concentration and bubbles scattering on photobiological hydrogen production in the close plane-parallel PBRs.

To the best of our knowledge, few studies have investigated the quantitative relationship between H_2 production performance and working conditions in a variable light intensity PBR hydrogen production system using the surface fitting method proposed. In the present study, the surface fitting can be converted into a curve fitting by the improved surface fitting, so the form of relational expression can be determined more easily. Accurate relational expressions are useful for the operation,

performance optimization and forecast of PBR in the application. Therefore, the objective of the present study was to obtain relational expressions about the performance and working conditions of the PBR system, a variable light intensity system, and provide a method to obtain the relational expressions of various PBR systems.

2. Models and Methods

2.1. Penetration of LED Light in the PBR

2.1.1. Model of Radiative Transfer

There is no doubt that the establishment of the radiative transfer model is an important part of numerical simulation in studying microalgae photobiological H_2 production in a PBR. In the present study, a plane-parallel photobioreactor of thickness L could be simplified as shown in Figure 1. The reactor contains the C. reinhardtii CC125 at concentration X with respect to the total volume of the reactor, kg dry cell/m^3. As Figure A1 in Appendix A shows, the microalgae absorption coefficient of wavelength range of 400–500 nm is higher, and it means that microalgae can utilize more light energy in this spectral range than in other spectral ranges. Thus, the adjustable blue light emitting diode (LED) lamps (the LED lamps have several bulbs controlled by power, and the incident radiation of each bulb can be measured by the blackbody furnace method, as in reference [9]) were selected as the light source. Taking the need to simplify the PBR system into account, the LED light lamps can be considered a point light source uniformly placed above the PBR. Moreover, the spectral absorption coefficient of microalgae is larger than that of pure water, which is shown in Appendix A in Figure A2 in the visible light spectrum, so the effects of the liquid phase were not considered. The reactor was illuminated only from the top with diffuse intensity $I_{in,\lambda}$, W/m^2/sr/nm. The PBR commonly works at a temperature of 292–298 K, so the emission of dispersion media in the reactor and the self-emitting of reactor walls are ignored [18]. Both the liquid phase and the microalgae absorb LED light in the process of light penetration at the PBR, and the microalgae scatter the LED light anisotropically. Hence, the one-dimensional steady-state radiative transfer equation (RTE) can be written according to [2]:

$$s \cdot \frac{\partial I_\lambda(z,\boldsymbol{s})}{\partial z} = -\kappa_{eff,\lambda} I_\lambda(z,s) - \sigma_{eff,\lambda} I_\lambda(z,s) + \frac{\sigma_{X,\lambda}}{4\pi} \int_{4\pi} I_\lambda(z,s_i)\Phi_{X,\lambda}(s_i,s)d\Omega_i \quad (1)$$

where $I_\lambda(z,s)$ denotes the light intensity at location z in direction s, W/m^2/sr/nm. $\Phi_{X,\lambda}$ denotes the scattering phase function of the microalgae. $\sigma_{X,\lambda}$ is the spectral scattering coefficient of the microalgae, m^{-1}. $\kappa_{eff,\lambda}$ and $\sigma_{eff,\lambda}$ are the effective spectral absorption and scattering coefficients, respectively, expressed in m^{-1}. It can be written as:

$$\kappa_{eff,\lambda} = \kappa_{L,\lambda}\left(1 - \frac{X}{\rho_m}\right) + A_{abs,\lambda}X \quad (2)$$

$$\sigma_{eff,\lambda} = \sigma_{X,\lambda} = S_{sca,\lambda}X \quad (3)$$

where ρ_m is the density of C. reinhardtii, equal to 1350 kg/m^3. The absorption coefficient of the liquid phase is denoted $\kappa_{L,\lambda}$, m^{-1}. In experiments, C. reinhardtii usually grown in tris-acetate-phosphate-sulfate (TAP + S) medium and produces hydrogen in sulfur-deprived medium (TAP-S, sulfate was substituted with an equivalent amount of chloride salts) [19]. In our simulation, considering that the optical properties of the liquid phase are similar to pure water, and the spectral absorption coefficient of water [20] is shown in Appendix A in Figure A2. $A_{abs,\lambda}$ and $S_{sca,\lambda}$ denote the mass absorption cross-section of microalgae and the mass scattering cross-section of microalgae, respectively, expressed in m^2/kg. In addition, the term $A_{abs,\lambda}X$ in Equation (2) and $S_{sca,\lambda}X$ in Equation (3) are the spectral absorption coefficient of microalgae $\kappa_{X,\lambda}$ expressed in m^{-1} and the spectral scattering coefficient of microalgae $\sigma_{X,\lambda}$, respectively. The mass absorption and scattering cross-sections $A_{abs,\lambda}$

and $S_{sca,\lambda}$ can be calculated from the absorption and scattering cross-sections of the microalgae $C_{abs,\lambda}$ and $C_{sca,\lambda}$ according to [21]:

$$C_{abs,\lambda} = A_{abs,\lambda} V_{32} \rho_m (1 - X_w) \tag{4}$$

$$C_{sca,\lambda} = S_{sca,\lambda} V_{32} \rho_m (1 - X_w) \tag{5}$$

where V_{32} denotes that the mean particle volume is 3.36×10^{-16} m^3 for C. reinhardtii CC 125. $C_{abs,\lambda}$ and $C_{sca,\lambda}$ are expressed in m^2. Moreover, X_w was taken as 0.78 for C. reinhardtii. Finally, the spectral absorption and scattering cross-sections of C. reinhardtii CC 125 [21] are shown in Appendix A in Figure A1.

The boundary conditions are of great importance in solving the RTE in simulation. Assuming that the boundary of PBR is completely transmitted, and mismatch of the refractive index between the disperse medium and air is neglected, the PBR is considered to be horizontally placed. As can be seen in Figure 1, illumination only is from the top with a diffuse light, and the back surface is considered to be cold and black. Thus, the boundary conditions of RTE can be written as:

$$\begin{aligned} I_\lambda(0,\theta) &= \frac{E_{in,\lambda}}{2\pi} = I_{in,\lambda} \quad \text{for} \quad 0 \le \theta < \frac{\pi}{2} \\ I_\lambda(L,\theta) &= 0 \qquad\qquad\quad \text{for} \quad \frac{\pi}{2} \le \theta < \pi \end{aligned} \tag{6}$$

where $E_{in,\lambda}$ is the total emissive power of LED light at λ, W/m^2/nm. As shown in Appendix A in Figure A3, the spectral emissive power of blue LED light is measured by [8]. In order to simplify the calculation, according to the box model [22] (pp. 362–371), the absorption and scattering cross-sections of the microalgae and the spectral absorption coefficient of water are approximated by the average value within the wavelength range from 400 nm to 500 nm in the PBR of the blue LED light source.

The Henyey-Greenstein (*HG*) phase function can be used to approximate the scattering phase function of microalgae in PBR given by [18]:

$$\Phi_{HG}(\Theta) = \frac{1 - g^2}{[1 + g^2 - 2g\cos\Theta]^{3/2}} \tag{7}$$

where Θ denotes the scattering angle, rad. g is the asymmetric factor of microalgae equal to 0.9834 for C. reinhardtii [12].

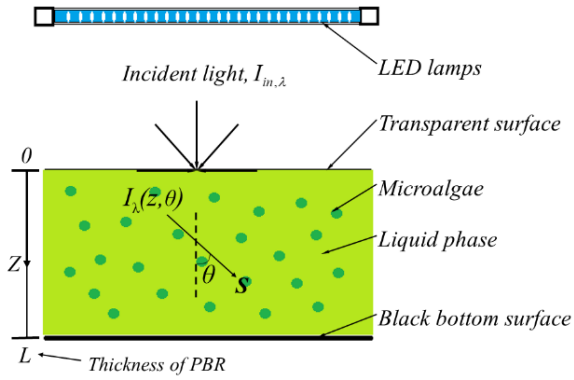

Figure 1. The schematic of the photobioreactor system.

2.1.2. Solution Method of Steady RTE

In this paper, the finite volume method (FVM) is used to solve the steady RTE in the PBR [18]. Moreover, to make the problem mathematically trackable, the following assumptions are made [18]:

1. The radiative transfer is an 1D steady-state process which is typical and widely used in numerical simulation of PBR.

2. Under the action of a magnetic stirrer, the distribution of C. reinhardtii CC 125 cells is uniform in the PBR, and the effect of convection is ignored.
3. The effect of bubbles is ignored, and the liquid phase can be considered to be pure water, which is cold, absorbing, and non-scattering.
4. Mismatch of the refractive index between the disperse medium and air is neglected.
5. The top surface and bottom surface of PBR are non-reflecting and black, respectively.

Finally, according to the calculation, the radiative characteristics of C. reinhardtii CC 125 cells and liquid phase are shown in Table 1.

Table 1. The radiative characteristics of C. reinhardtii CC 125 cells and liquid phase.

Wavelength	**λ (nm)**	**400–450**
Liquid	$\kappa_{L,\lambda} \times 10^3 \left(\mathrm{m}^{-1}\right)$	35.9
Microalgae	$A_{abs}\left(\mathrm{m}^2/\mathrm{kg}\right)$	266.17
-	$S_{sca}\left(\mathrm{m}^2/\mathrm{kg}\right)$	415.184

2.2. Photobiological H_2 Production Kinetics Model of PBR

The hydrogen production process of PBR can be simulated by the photobiological H_2 production kinetics model. Considering the effect of photo-inhibition on the hydrogen production process, the Michaelis-Menten model has proven to be highly effective as a model of simulation [23], and it has been applied extensively. Further, there is an experimental model of the PBR system in reference [9], which is highly similar to the simulation model in this paper, and Figure 2 shows that the hydrogen production simulation of C. reinhardtii GY-D55 using the Michaelis-Menten equation was compared with an experiment illuminated with a blue LED lamp [9] (the data in Figure 2 is reprinted from Reference [9]).

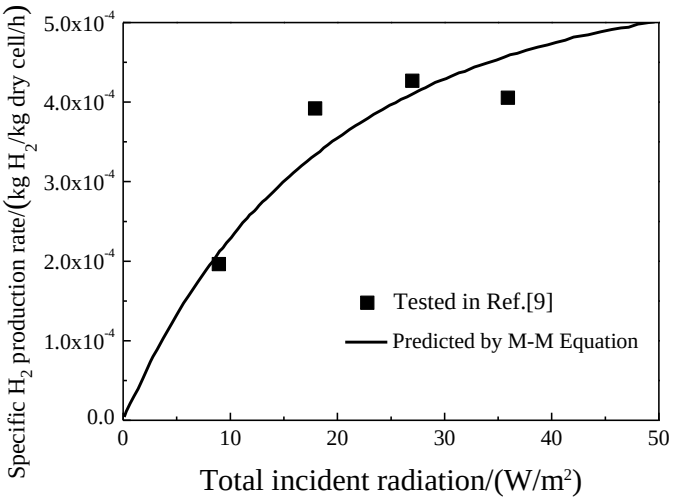

Figure 2. Hydrogen production simulation of C. reinhardtii GY-D55 by the Michaelis-Menten equation was compared with an experiment illuminated with a blue light emitting diode (LED) lamp [9].

Thus, the Michaelis-Menten equation is used to describe the relationship between local incident radiation and hydrogen productivity in the present study. It was proposed as follows [24] (pp. 254–268):

$$\pi_{H_2}(z) = \pi_{H_2,max} \frac{E(z)}{K_G + E(z) + E^2(z)/K_I} \tag{8}$$

where $E(z)$ is the local incident radiation, W/m^2; $\pi_{H_2}(z)$ presents the local specific hydrogen production rate; K_G and K_I are the saturation and inhibition irradiation for hydrogen production equal to 25 W/m^2 and 120 W/m^2, respectively [12]; $\pi_{H_2,max}$ is the maximum specific hydrogen production rate, kg H_2/kg dry cell/h. As mentioned above, in order to overcome the oxygen inhibition of hydrogenase, assuming that C. reinhardtii CC125 is cultured in a sulfur-deprived medium. Berberoglu and Pilon [12] obtained the maximum specific hydrogen production rate, which is equal to 5.51×10^{-4} for sulfur-deprived cells according to experimental data C. reinhardtii by sulfur-deprived cultures in reference [19], and applied it to numerical simulation of C. reinhardtii CC125.

The total photosynthetic effective hydrogen production rate in plane-parallel PBR can be written as:

$$m_{H_2} = A_s \int_L \pi_{H_2}(z) X(z) dz \tag{9}$$

where A_s is the irradiated surface area of PBR equal to 1 m^2 in our study. L is thickness of the PBR equal to 0.1 m. Finally, the accuracy of the radiative characteristic and the characteristics parameters of hydrogen production kinetics used to our model has already proven by experimental data. Thus, this paper did not verify the accuracy of radiative transfer model and photobiological H_2 production kinetics model by experiment.

2.3. Performance Parameters of PBR

The performance of a PBR system depends on working conditions of PBR (i.e., light intensity, cell concentration, microorganism species, temperature, culture medium pH, CO_2 content, as well as size and structure of PBR, to name a few), and different PBR systems have different variable parameters, structures and mechanisms. Although an investigation of all factors and all kinds of PBR systems is beyond the scope of this work, an approximated method is provided to relate all of these factors with the performance of PBR. As a matter of fact, in practical applications, the light intensity of a PBR system using an LED light source can be adjusted. In addition, the concentration of cells in the PBR varies with cellular activities. Moreover, the size and structure of PBRs are fixed at the beginning of manufacture. Thus, only the variation of light illumination and microalgae concentration affect the performance of the isothermal system when the variations in the culture medium pH and CO_2 content were ignored.

The performance parameters were evaluation parameters of a system in a certain working condition. The total photobiological hydrogen production rate was a basic performance parameter mentioned in the paragraph above. Further, the efficiency of hydrogen production is as important as the rate of hydrogen production generally. So, the conversion efficiency of light energy to hydrogen energy is an indispensable performance parameter of the PBR system. It can be calculated by:

$$\eta_{H_2} = \frac{\Delta G_0 m_{H_2}}{M_{H_2} A_s E_{tot}} \tag{10}$$

where ΔG_0 denotes the standard-state free energy of formation of H_2 from water splitting reaction, which is 236337 J/mol at the temperature of 303 K. M_{H_2} is the molecular mass of hydrogen equal to 2.016×10^{-3} kg/mol. E_{tot} presents the total incident radiation of LED light, W/m^2.

As shown in Figure 3, it can be seen that when the concentration of microalgae is constant in the PBR, the total hydrogen production rate of the PBR system increases with the enhancement of light intensity in the photo-promoting zone, and an opposite trend presents itself in the photo-inhibiting zone. It is apparent that there is a working condition point of maximum total photosynthetic effective hydrogen production rate at the boundary of photo-inhibiting and photo-promoting zones. In order to present the potential of hydrogen production at a certain cell concentration, the ratio of the total hydrogen production rate in the photo-promoting zone and the maximum total hydrogen production

rate at a certain microalgae concentration X is defined as the dimensionless hydrogen production rate at microalgae concentration X as a performance parameter. It can be written as:

$$\alpha_X = \frac{m_{H_2,X}}{m_{H_2,X,max}} \tag{11}$$

where α_X is the dimensionless hydrogen production rate at microalgae concentration X. $m_{H_2,X,max}$ denotes the maximum total hydrogen production rate of the microalgae at a certain microalgae concentration X, kg/h. Moreover, the hydrogen production thrust coefficient expressed in s^2 is defined to indicate the difficulty of conversion of light energy into hydrogen energy. This performance parameter can be written:

$$\xi_X = \frac{dm_{H_2,X}}{dE_{tot}} \tag{12}$$

where $m_{H_2,X}$ denotes the total photosynthetic effective hydrogen production rate in the PBR at microalgae concentration X in the photo-promoting zone, in kg/h. Obviously, the larger ξ_X is, the more easily the total photosynthetic effective hydrogen production rate increases when the light intensity is increasing, and vice versa.

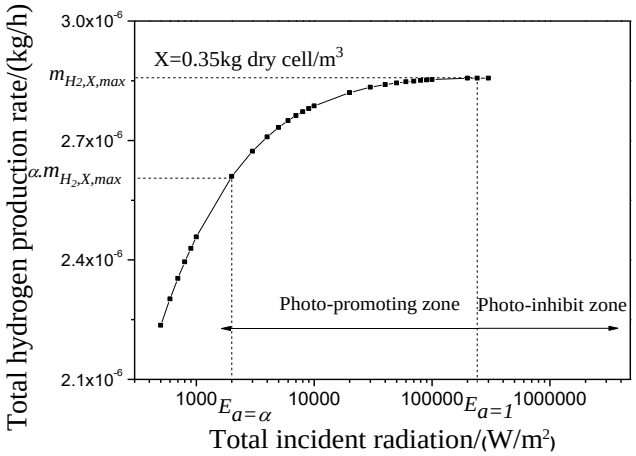

Figure 3. Photo-promoting and photo-inhibit zone.

2.4. Fitting the Performance Curves and Surfaces of PBR

2.4.1. Fitting Curves Based on Improved Quantum-Behaved Particle Swarm Optimization Algorithm

In order to facilitate the engineering applications of the performance curve (i.e., the curve relating system performance to working conditions) of the PBR, it is necessary to fit the performance curve generally. In the present study, the sum of squares of relative errors is considered as the undetermined function optimized in the curve fitting process. It can be written as:

$$RE = \sum_{i=1}^{n} \left(\frac{y_i - \Gamma(x_i)}{y_i} \right)^2 \tag{13}$$

where (x_i, y_i) is the data point on the curve; $\Gamma(x)$ is the objective function of the fitting curve. The coefficient of the function $\Gamma(x)$ can be determined when the value of RE is the minimum value. The improved quantum-behaved particle swarm optimization (IQPSO) algorithm presented in [25] is used to optimize the undetermined function RE in our study. The detail of the IQPSO available in reference [25] will not be repeated here. The flow chart of curve fittings based on the IQPSO is shown in Figure 4.

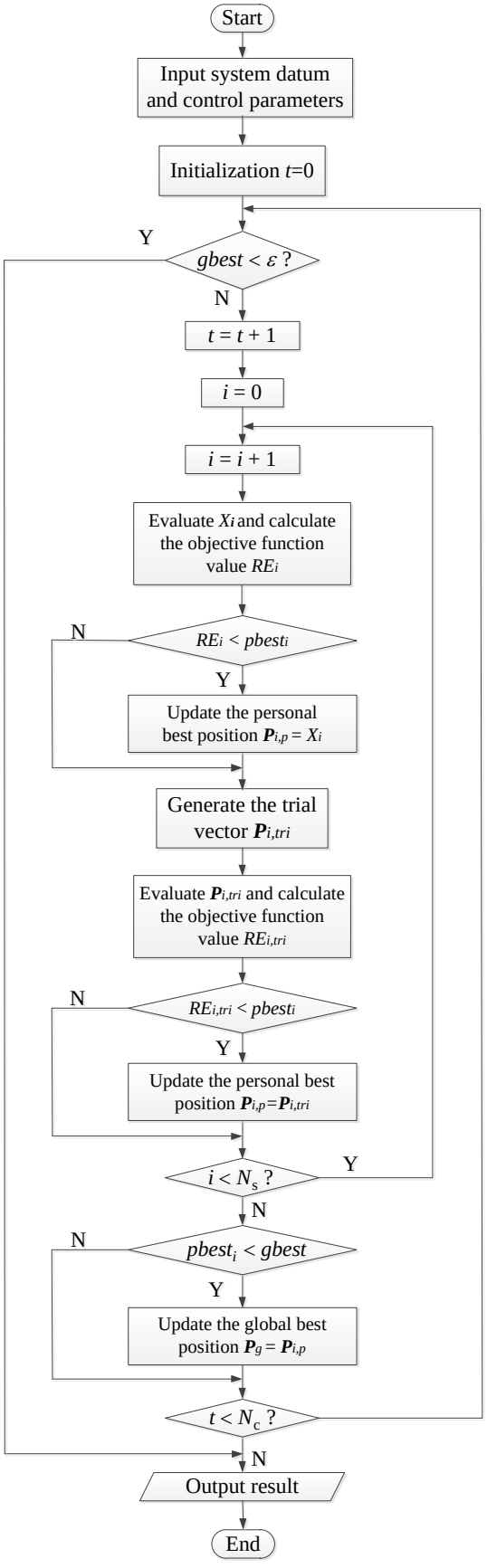

Figure 4. The flow chart of curves fitting based on improved quantum-behaved particle swarm optimization.

2.4.2. Surface Fitting Based on the Method of Curve Fitting

Fitting the performance surface (i.e., the multi-dimensional surface of relating system performance with working conditions) is necessary to obtain the relational expressions about various performance parameters and working conditions. Moreover, in order to simplify the selection of the fitting relational expressions, the curve fitting method is used to fit the surface. The flow chart of the surface fitting is shown in Figure 5. For a multidimensional performance surface, the relationship between several parameters can be presented as follow:

$$A = \Psi(B_1, B_2, B_3, ..., B_n) \tag{14}$$

where A and B_i $(i = 1, 2, 3, ..., n)$ denote the parameters. Ψ is an undetermined relational expression.

Step 1. Select a relational expression (such as $A = \Psi(B_1, P(i))$ where $P(i)$ $(i = 1, ...)$ is an undetermined coefficient vector) to fit the scatter plot about A and B_1 at several different B_2 which are in the range of values.

Step 2. Select a relational expression (such as $P(i) = f_1(B_2, Q(i, j))$ where $Q(i, j)$ $(j = 1, ...)$ is an undetermined coefficient matrix) to fit the scatter plot about $P(i)$ $(i = 1, ...)$ and B_2 at several different B_3 which are in the range of values.

Step 3. Select a relational expression (such as $Q(i, j) = f_2(B_3, R(i, j, k))$ where $R(i, j, k)$ $(k = 1, ...)$ is an undetermined coefficient matrix) to fit the scatter plot about $Q(i, j)$ $(j = 1, ...)$ and B_3 at several different B_4 which are in the range of values.

And so on, the relational expression can be written as:

$$A_{sf} = \Psi(B_1, f_1(B_2, f_2(B_3, f_3(B_4, ...)))) \tag{15}$$

In this paper, only the three-dimensional performance surface was fitted, since only the variation of light illumination and microalgae concentration was considered in the PBR system. The method of fitting the multidimensional performance surface is proposed as a reference for complex working conditions. Finally, the relative error matrix was used to represent the quality of the surface fitting, and it can be written as:

$$\boldsymbol{REM} = \frac{\left|A_{sf} - A\right|}{|A|} \tag{16}$$

where A_{sf} and A are the total incident radiation obtained from the relational expression and the simulation, respectively.

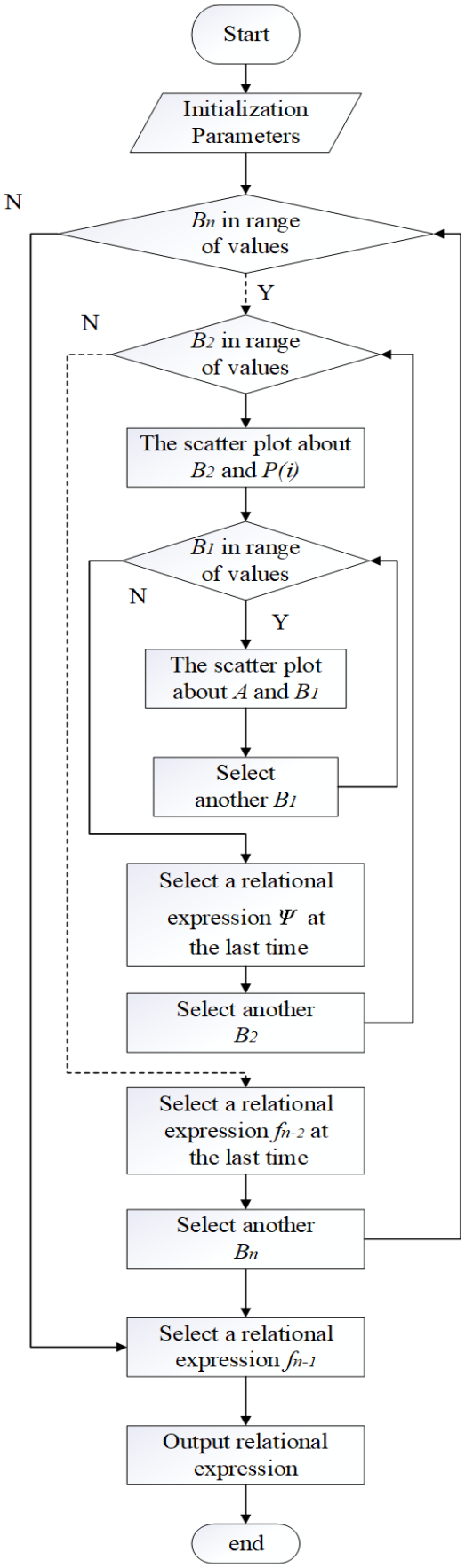

Figure 5. The flow chart of fitting surface based on the method of curve fitting.

3. Results and Discussions

3.1. Effect of Working Conditions of PBR System on Hydrogen Production Thrust Coefficient

Before analyzing the variation of other performance parameters in the system with working conditions, it is essential to study the influence of microalgae concentration and light intensity on the hydrogen production thrust coefficient. It can be seen in Figure 6 that the hydrogen production thrust coefficient of PBR increased with the increase of microalgae concentration. This is due to the fact that at a same light intensity, microalgae cells with lower concentration in PBR are more susceptible to the effects of the photoinhibition effect, compared with microalgae cells in larger concentrations. Therefore, when the concentration of microalgae is low, the light energy can hardly be converted into hydrogen energy because of the strong photo-inhibition effect, that is, the hydrogen production thrust coefficient is smaller. Moreover, with the increase in total incident radiation, the hydrogen production thrust coefficient in PBR decreased continuously. Because the number of photo-inhibited microalgae cells in PBR increases with the increase of light intensity, it is more difficult to convert light energy into hydrogen energy (i.e., the hydrogen production thrust coefficient is smaller).

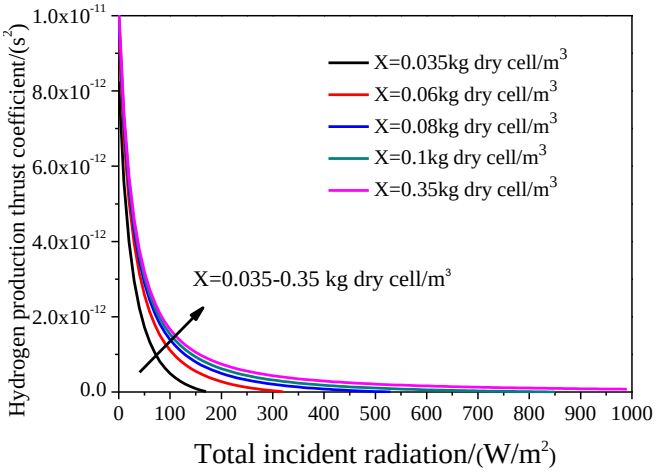

Figure 6. The curves of hydrogen production thrust coefficient varying with light intensity and microalgae concentration.

3.2. Operation Guideline for Variable Light Intensity PBR System

Variable light intensity PBR systems have great potential to improve performance and save energy. It is of great significance to study the relationship between the concentration of microalgae, the light intensity, and the performance of PBR. Figure 7 shows the curves for total incident radiation and the total hydrogen production rate varying with the concentration of microalgae at $\alpha = 1$. With the increase in microalgae concentration, the corresponding light intensity and hydrogen production rate were enhanced. In addition, with the increase in microalgae concentration, the growth rate of light intensity increased, and the growth rate of hydrogen production rate decreased. According to Figure 7, the higher the concentration of microalgae and the total incident radiation are, the larger the hydrogen production thrust coefficient and the slope of the hydrogen production thrust coefficient curve. When $\alpha = 1$, the hydrogen production thrust coefficient was 0. Therefore, the higher the concentration of microalgae, the larger the light intensity, the more difficult it is to drop the hydrogen production thrust coefficient to 0. As a result, the explosive growth occurred with higher concentrations of microalgae. Moreover, with the increase in light intensity, the hydrogen production thrust coefficient decreased constantly due to the photo-inhibition effect. As a result, the increase of hydrogen production rate became smaller and smaller. Figure 8a,b shows that when the concentration of microalgae was constant, conversion efficiency of light energy to hydrogen energy was improved and the light intensity of LED decreased with the decreasing α. Therefore, when the requirements of total photosynthetic

effective hydrogen production rate and conversion efficiency of light energy to hydrogen energy are determined, the relationship between the intensity of LED light and the concentration of microalgae can be determined in the process of PBR operation.

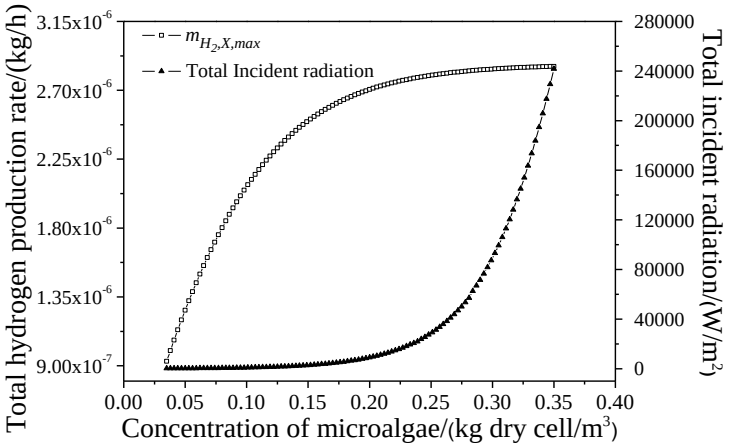

Figure 7. The curves of total incident radiation and total hydrogen production rate varying with the concentration of microalgae at $\alpha = 1$.

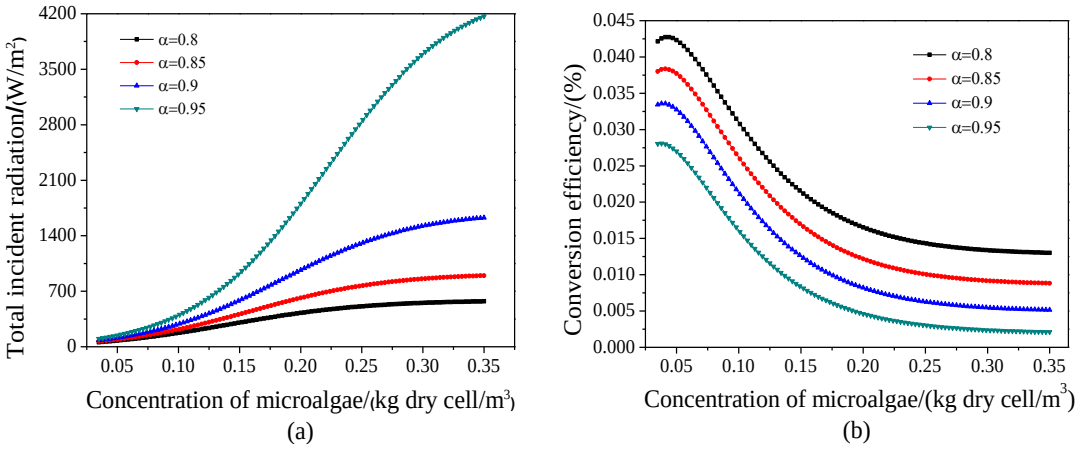

Figure 8. (**a**) The curves of total LED incident radiation with the concentration of microalgae and the dimensionless hydrogen production rate; (**b**) the curves of conversion efficiency of light energy to hydrogen energy with the concentration of microalgae and the dimensionless hydrogen production rate.

3.3. PBR Performance Surfaces and Curves Fitting

In engineering applications, the accurate quantitative relationship between performance parameters and working conditions is obviously more convenient in operation, performance optimization and forecasting of a PBR system. Therefore, the relational expressions were obtained with the fitting performance surface or curve in this section. Figure A4 in Appendix A shows the relative error between the curve of total hydrogen production rate varying with microalgae concentration at $\alpha = 1$ and the fitting curve obtained by the IQPSO curve fitting method. It can be seen that the maximum relative error did not exceed 2%. The fitting relational expression is as follows:

$$m_{H_2,max,cf} = \exp\left(\sum_{i=1}^{7} P_{m_{H_2}}(i) X^{(i-1)}\right) \quad (17)$$

where X is between 0.035 and 0.35 kg dry cells/m^3. $P_{m_{H_2}}(i)$ is shown in Appendix A in Table A1. According to the definition of α, the relational expressions of total hydrogen production rate, dimensionless hydrogen production rate, and microalgae concentration are as follows:

$$m_{H_2,cf} = \alpha \cdot \exp(\sum_{i=1}^{7} P_{m_{H_2}}(i) X^{(i-1)}) \tag{18}$$

The performance surface of the light intensity varying with the dimensionless hydrogen production rate α (0.96–0.998) and the microalgae concentration X (0.035–0.35 kg dry cell/m^3), shown in Figure 9a, was fitted as an example in this section. According the section above, the larger α was, the smaller the hydrogen production thrust coefficient and conversion efficiency of light energy to hydrogen energy were. Thus, α was no more than 0.998 in the present study. For the three-dimensional surface fitting, the surface is converted to the family of curves, as shown in Figure 9b. In addition, according to the characteristics of the family of curves, a same form of relational expression is determined to fit each curve in the curve family. The fitting relational expression chosen in this example is as follows:

$$\left(E_{tot,sf} = \exp(\sum_{i=1}^{n} p(i) X^{(n-i)}) \right)_{\alpha=a} \tag{19}$$

where $p(i)$ is an undetermined coefficient; n denotes the number of polynomial terms in the exponential part of the relational expression equal to 5 in this example; $(...)_{\alpha=a}$ denotes the relational expression of the curve of $\alpha = a$ in the family of curves. Then, the scatter plot of α and $p(i)$ obtained from the above was fitted for obtaining the relational expression, and it can be written as:

$$p(i) = f_i(\alpha) \tag{20}$$

where $f_i(\alpha)$ can be obtained according to the characteristics of the scatter distribution. The scatter plot of α and $p(i)$ and the curve of function $f_i(\alpha)$, for this example, are shown in Figure 10a–e. In this example,

$$f_i(\alpha) = \sum_{j=1}^{5} Q_{E_{(0.96-0.998)}}(i,j) \alpha^{(n-j)} \tag{21}$$

where $Q_{E_{(0.96-0.998)}}(i,j)$ is the coefficient matrix of surface relational expressions shown in Appendix A in Table A2. Finally, Substituting Equation (21) into Equation (19) yields the surface relational expression, as follows:

$$E_{tot,sf} = \exp(\sum_{i=1}^{5} \sum_{j=1}^{5} Q_{E_{(0.96-0.998)}}(i,j) \alpha^{(5-j)} X^{(5-i)}) \tag{22}$$

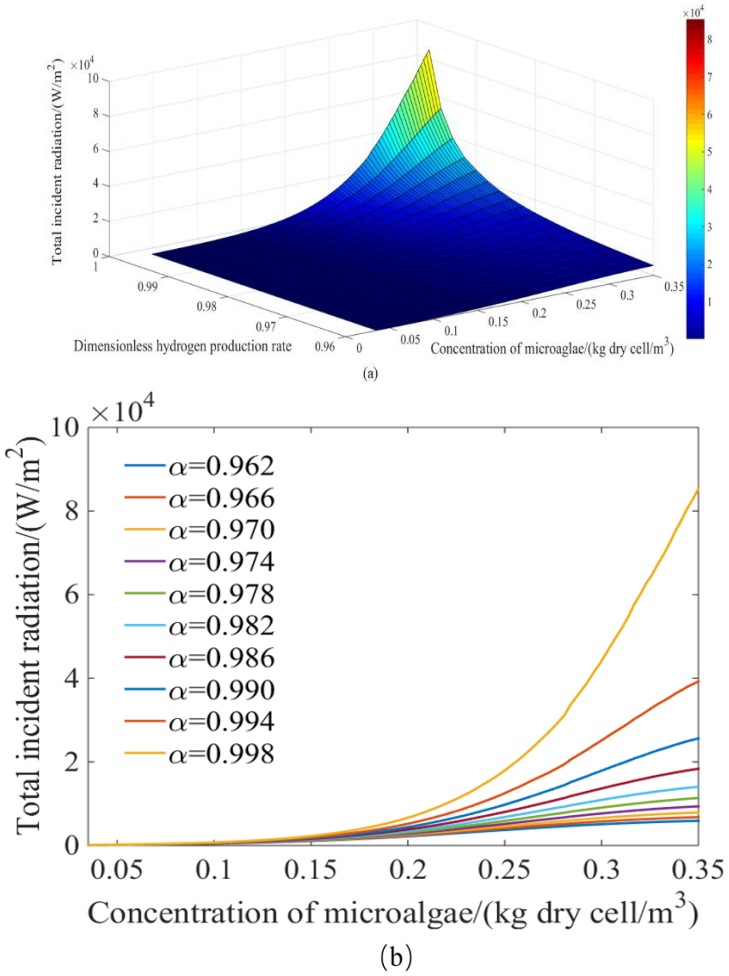

Figure 9. (**a**)The performance surface of total incident radiation varying with the dimensionless hydrogen production rate (0.96–0.998) and the microalgae concentration; (**b**) the family of curve converted from Figure 9a.

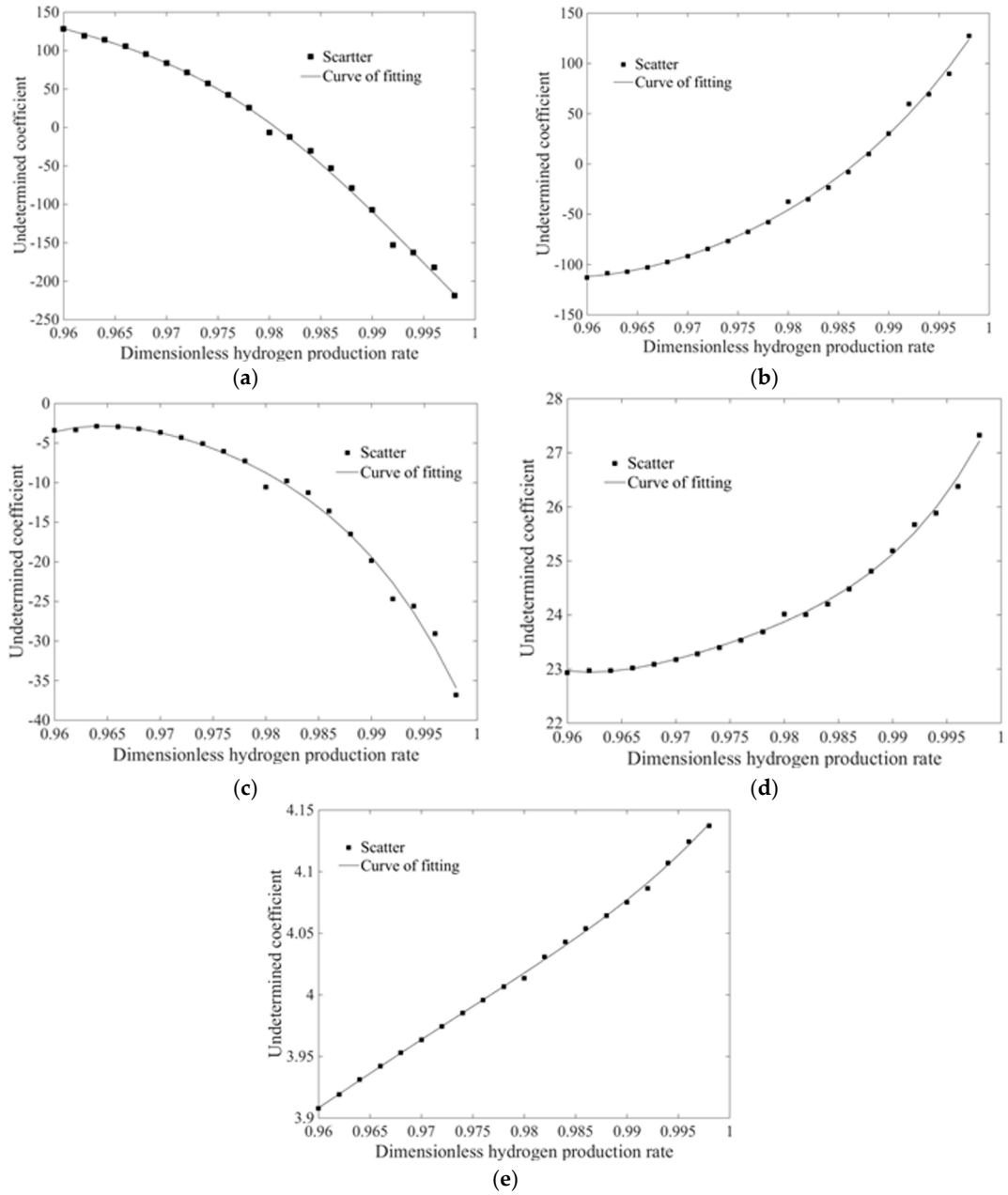

Figure 10. (**a**) The scatter plot of α and $p(1)$ and the curve of function $f_1(\alpha)$; (**b**) the scatter plot of α and $p(2)$ and the curve of function $f_2(\alpha)$; (**c**) the scatter plot of α and $p(3)$ and the curve of function $f_3(\alpha)$; (**d**) the scatter plot of α and $p(4)$ and the curve of function $f_4(\alpha)$; (**e**) the scatter plot of α and $p(5)$ and the curve of function $f_5(\alpha)$.

The relative error matrix for this example is shown in Appendix A in Figure A5. As can be seen in Figure A5 in Appendix A, the relative error of the surface relational expression obtained by this method was within an acceptable range. The performance surface of the light intensity with the dimensionless hydrogen production rate α (0.1–0.96) and the microalgae concentration X (0.035–0.35 kg dry cell/m^3) is shown in Figure 11. The smaller α was, the smaller the hydrogen production rate and penetration depth of light were. Therefore, the dimensionless hydrogen production rate was set as $\alpha \geq 0.1$. In this paper, the fitting relational expression of Figure 11 can be written as:

$$E_{tot,sf} = \exp\left(\sum_{i=1}^{5}\sum_{j=1}^{8} Q_{E_{(0.1-0.96)}}(i,j)\alpha^{(8-j)}X^{(5-i)}\right) \quad (23)$$

where $Q_{E_{(0.1-0.96)}}(i,j)$ is shown in Appendix A in Table A3. As shown in Appendix A in Figure A6, the maximum of the relative error matrix is 4%, which means that if the concentration of microalgae and hydrogen production rate is in that region mentioned above, there will be a relatively larger error between the numerical results and the fitting surface. However, the result was still acceptable, and it can be used to guide operation of the PBR system. According to the definition of conversion efficiency of light energy to hydrogen energy η_{H_2}, the relational expressions of η_{H_2}, α and X are as follow:

$$\eta_{H_2,f} = \begin{cases} 32564.071 \times \alpha \cdot exp\left(\sum_{i=1}^{7} P_{m_{H_2}}(i) X^{(1-i)} - \sum_{i=1}^{5} \sum_{j=1}^{8} Q_{E_{(0.1-0.96)}}(i,j) \alpha^{(8-j)} X^{(5-i)} \right) \text{ for } 0.10 \le \alpha \le 0.96 \\ 32564.071 \times \alpha \cdot exp\left(\sum_{i=1}^{7} P_{m_{H_2}}(i) X^{(1-i)} - \sum_{i=1}^{5} \sum_{j=1}^{5} Q_{E_{(0.96-0.9698)}}(i,j) \alpha^{(5-j)} X^{(5-i)} \right) \text{ for } 0.96 \le \alpha < 0.998 \end{cases} \quad (24)$$

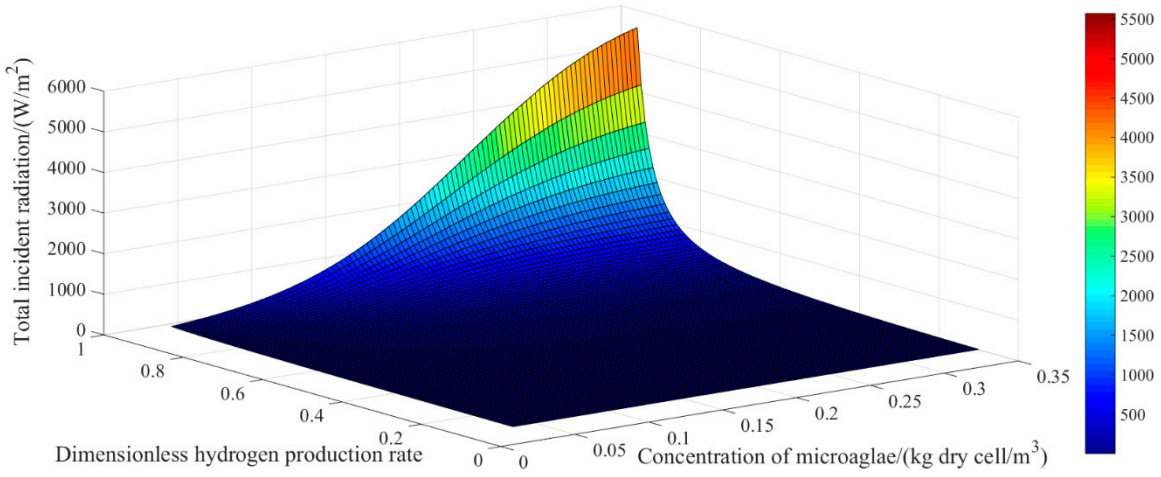

Figure 11. The performance surface of total incident radiation with the dimensionless hydrogen production rate (0.1–0.96) and the microalgae concentration.

4. Calculating Performance Surface of Hydrogen Production

To verify the accuracy of the above expressions, the performance surface of hydrogen production (i.e., the surface of total hydrogen production rate varying with light intensity and microalgae concentration) was calculated by applying the above quantitative relationship and comparing with the surface of hydrogen production obtained by simulation.

Figure 12 shows the surface of hydrogen production in calculating where the black line represents the dimensionless hydrogen production rate $\alpha = 0.998$. In addition, the surface of hydrogen production of the simulation is shown in Figure 13. As seen in Appendix A in Figure A7, the maximum of the relative error matrix did not exceed 2%. Thus, the accuracy of the above relational expressions is satisfying. It is demonstrated that the improved curve and surface fitting can be applied to quantitative research of PBR performance, and it is of great significance in forecasting and optimizing PBR performance quickly and precisely.

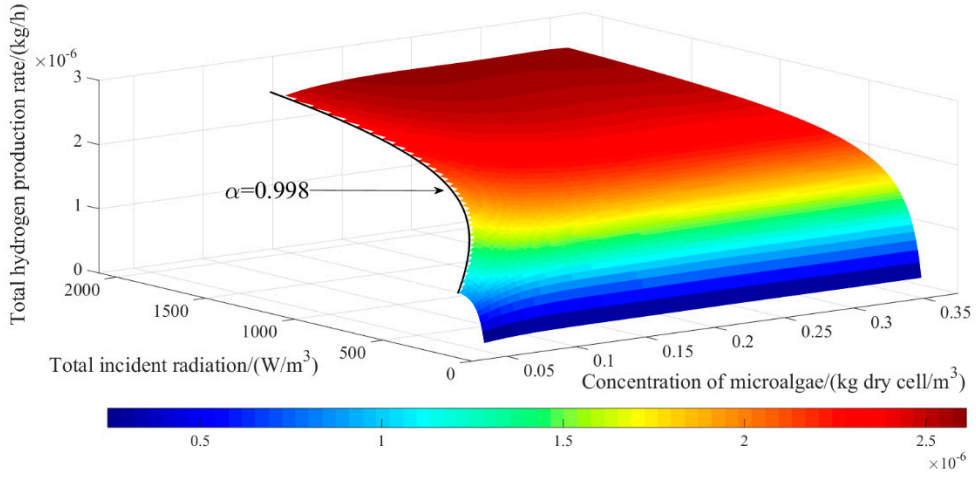

Figure 12. The surface of hydrogen production of fitting.

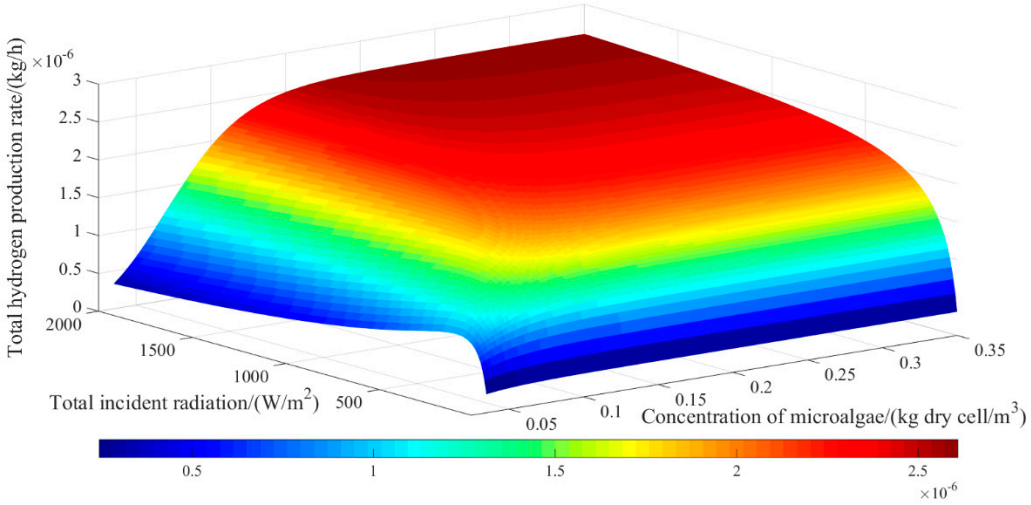

Figure 13. The surface of hydrogen production of simulation.

5. Conclusions

In the present study, taking a variable light intensity PBR system as an example, the performance of the PBR system was studied quantitatively. Meanwhile, the relational expressions about the performance and working conditions of variable light intensity PBR system have been obtained by surface fitting based on curve fitting. The following conclusions can be drawn:

1. For the C. reinhardtii CC125 ranging from 0.035 to 0.35 kg dry cell/m^3, the hydrogen production thrust coefficient of PBR increased with the increase in microalgae concentration and decreased with the increase in total incident radiation in the photo-promoting zone. This means that the higher the total incident radiation and the smaller microalgae the concentration, the more difficult it is to convert light energy to hydrogen energy.
2. In the variable light intensity PBR system, the dimensionless hydrogen production rate is of great significance to relate microalgae concentration with light intensity. By optimizing the dimensionless hydrogen production rate varying with light intensity, the performance of variable light intensity PBR systems can be effectively maintained (i.e., both hydrogen production rate and conversion hydrogen rate are satisfying) at different concentrations. In other words, the potential for hydrogen production of PBR determines the operation of the PBR system.
3. The performance surface was used to express the relationship of performance and working conditions. Moreover, the three-dimensional performance surface is fitted using the surface fitting

method based on curve fitting. It is demonstrated that this surface fitting method is easy, accurate and operable for a three-dimensional surface.

4. When it is necessary to study the performance of different PBR systems, the surface fitting method based on curve fitting can be used to fit the multi-dimensional performance surface and obtain the quantitative relationship, which can be used for the operation, forecast and optimization of PBR systems.

Finally, as mentioned above, with the increase in light intensity, hydrogen production of microalgae increased, however, energy conversion efficiency of microalgae decreased. Thus, it is difficult to weigh hydrogen production and energy conversion efficiency in variable light intensity PBR systems when microalgae concentration is variable. In this paper, the performance parameter α was defined to connect working condition parameters (including light intensity and microalgae concentrations) with PBR performance parameters (including hydrogen production and energy conversion efficiency) and used to keep the PBR system working efficiently. Moreover, the quantitative relationship between working conditions and the performance of a variable light intensity PBR system was obtained using an improved fitting surface method. It can be used to operate, optimize, and forecast the performance of the PBR system.

In practical applications, working conditions are more complicated. Future work should use more advanced empirical models of photobiological hydrogen production in order to take more factors into account.

Author Contributions: All authors have contributed equally to this work. Q.J., Z.H. and H.M. conceived the structure of paper; Methodology, Q.J. and Z.H.; investigation, Q.J.; writing-original draft preparation, Q.J., H.M.

Funding: This project is supported by the Fundamental Research Funds for the Central Universities, No. NS2018016.

Acknowledgments: A very special acknowledgement is made to the editors and referees who make important comments to improve this paper.

Conflicts of Interest: The authors declare no conflict of interest.

Nomenclature

A	a given parameter	ΔG_0	standard-state free energy of formation of H_2 from water splitting reaction, J/mol
$A_{abs,\lambda}$	spectral mass absorption cross-section, m^2/kg	ε	tolerance for minimizing the objective function in IQPSO algorithm
A_s	irradiated surface area of the PBR, m^2	η_{H_2}	conversion efficiency of light energy to hydrogen energy
B_i	a given parameter	θ	polar angle, rad
$C_{abs,\lambda}$	spectral absorption cross-section, m^2	Θ	scattering angle, rad
$C_{sca,\lambda}$	spectral scattering cross-section, m^2	κ	absorption coefficient, m^{-1}
E	incident radiation, W/m^2	λ	wavelength, nm
f_i	an undetermined relational expression	ξ	hydrogen production thrust coefficient, s^2
g	Henyey-Greenstein asymmetric factor	π_{H_2}	specific hydrogen production rate, kg H_2/kg dry cell/h
I_λ	spectral intensity, W/m^2/sr/nm	ρ_m	density of microalgae, kg/m^3
K_G	saturation irradiation, W/m^2	σ	scattering coefficient, m^{-1}
K_I	inhibition irradiation, W/m^2	Φ	scattering phase function
L	thickness of the PBR, m	Ω	solid angle, sr
M_{H_2}	molecular mass of hydrogen, kg /mol	*Subscripts*	
m_{H_2}	total photosynthetic effective hydrogen production rate, kg/h	*abs*	refer to absorption
N_s	total number of particles in IQPSO algorithm	*cf*	refer to curve fitting
N_c	user-defined iteration limit in IQPSO algorithm	*E*	refer to total incident radiation

$\boldsymbol{P}$	an undetermined coefficient vector (optimized by IQPSO algorithm) in relational expression obtained by fitting	eff	refer to effective radiation characteristics
$\boldsymbol{Q}, \boldsymbol{R}$	an undetermined coefficient matric in relational expression obtained by fitting	f	refer to fitting
RE	objective function in IQPSO algorithm	g	refer to global best position
$\boldsymbol{REM}$	relative error matric	HG	refer to Henyey-Greenstein
$\boldsymbol{S}$	unit vector into a given direction	in	refer to incident radiation
$S_{sca,\lambda}$	spectral mass scattering cross-section, m^2/kg	L	refer to liquid phase
t	iteration in IQPSO algorithm	max	refer to maximum
V_{32}	mean particle volume, m^3	m_{H_2}	refer to total photosynthetic effective hydrogen production rate
X	microalgae concentration, kg dry cell/m^3	p	refer to personal best position
$\boldsymbol{X}$	position of the particle in IQPSO algorithm	sca	refer to scattering
X_w	a constant in calculating of cross-section	sf	refer to surface fitting
Z	distance from the illuminated surface, m	tot	refer to total
Greek symbols		tri	refer to trial operation
α	dimensionless hydrogen production rate	X	refer to microalga concentration
Γ	objective function in curve fitting	λ	refer to wavelength

Appendix A

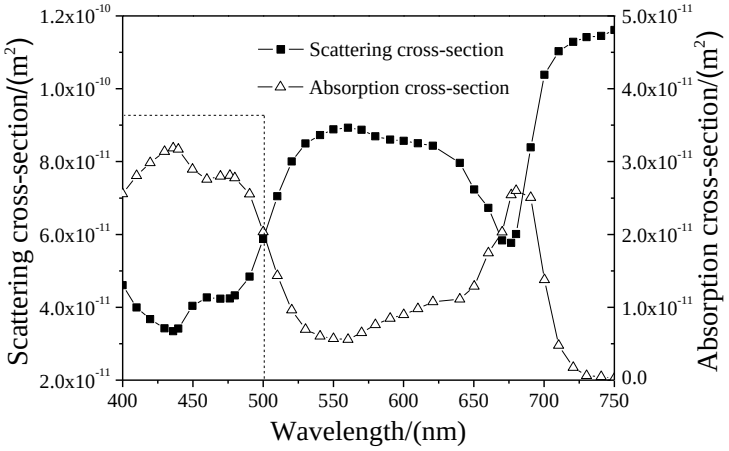

Figure A1. The spectral absorption and scattering cross-sections of C.reinhardtii CC 125 [21].

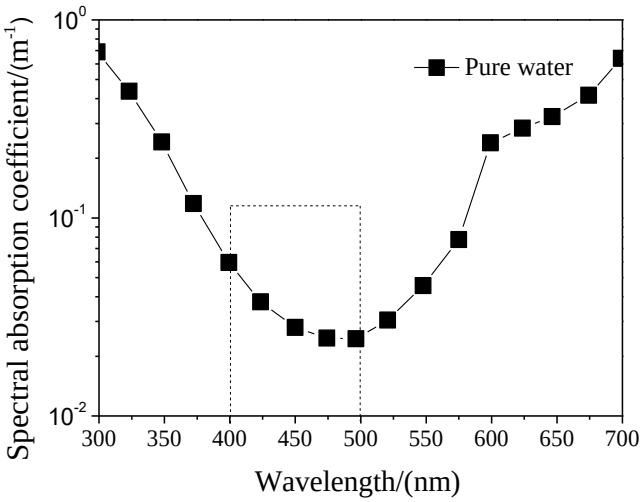

Figure A2. The spectral absorption coefficient of water [20].

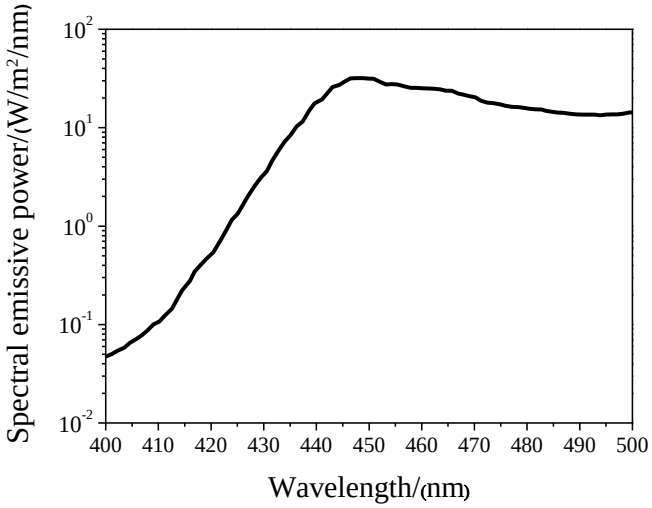

Figure A3. The spectral emissive power of blue LED light [9].

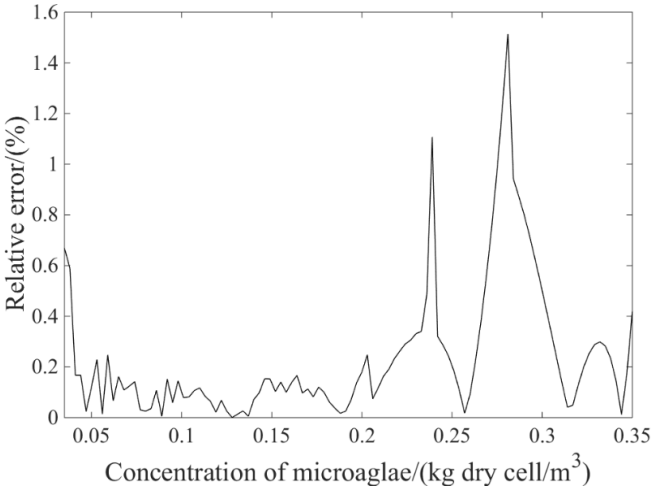

Figure A4. The relative error between the curve of the total hydrogen production rate varying with microalgae concentration at α = 1 and the fitting curve obtained using the improved quantum-behaved particle swarm optimization (IQPSO) curve fitting method.

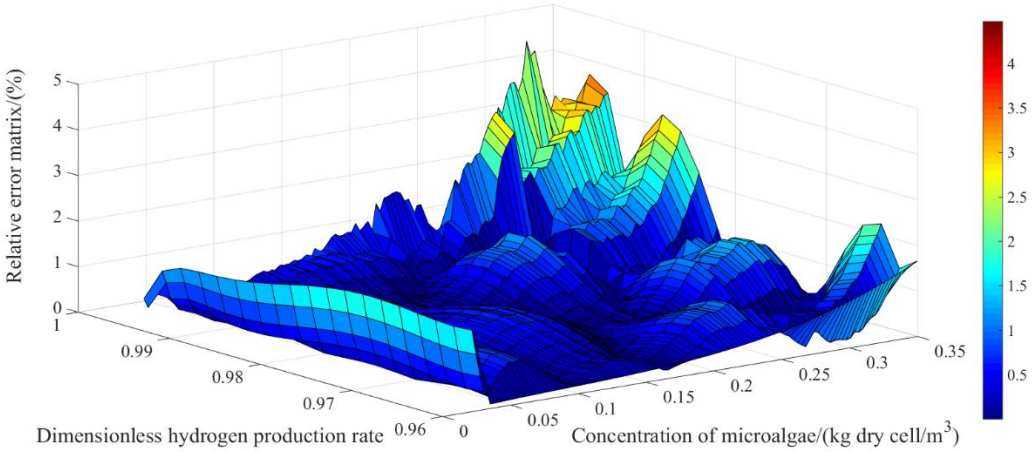

Figure A5. The relative error matrix about Figure 9a.

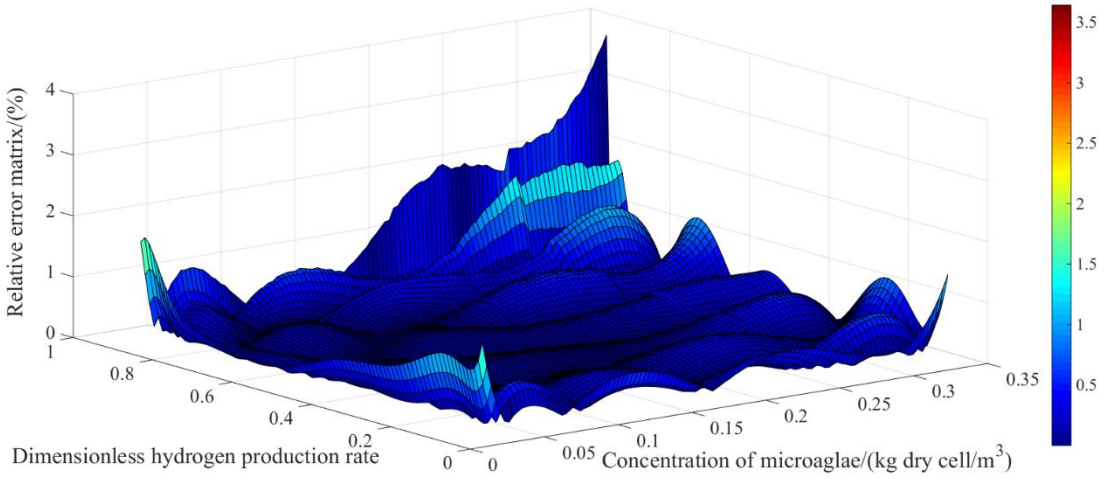

Figure A6. The relative error matrix about Figure 11.

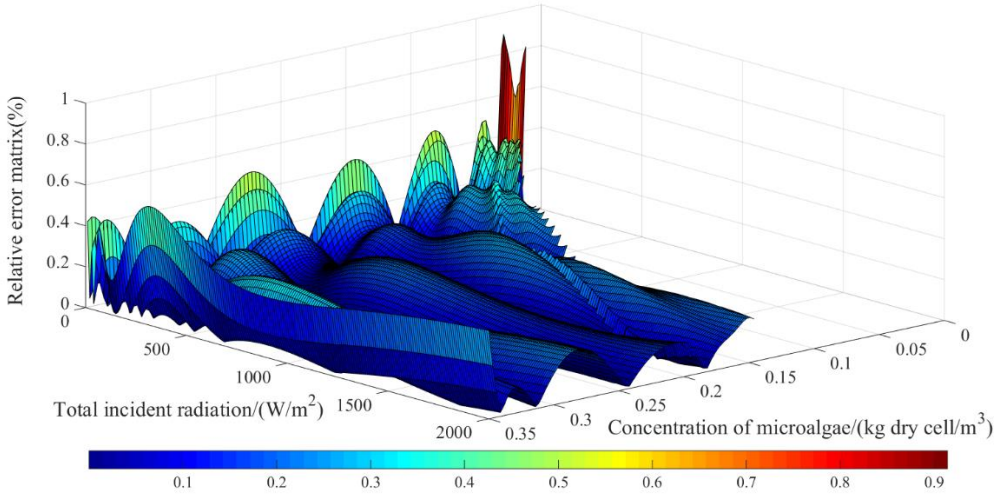

Figure A7. The relative error matrix about Figure 13.

Table A1. The coefficient matrix $P_{m_{H_2}}$.

$P_{m_{H_2}}(i)$	1	2	3	4	5	6	7
1	-1.506826×10^1	4.768869×10^1	-4.793022×10^2	2.794681×10^3	-9.452529×10^3	1.706414×10^4	-1.266231×10^4

Table A2. The coefficient matrix $Q_{E_{(0.96-0.998)}}$.

Q_E (i,j)	1	2	3	4	5
1	1.024569×10^8	-4.004445×10^8	5.867084×10^8	-3.819243×10^8	9.320317×10^7
2	6.107971×10^7	-2.373847×10^8	3.460882×10^8	-2.243250×10^8	5.454202×10^7
3	-2.325053×10^7	9.057460×10^7	-1.323360×10^8	8.594716×10^7	-2.093527×10^7
4	4.106285×10^6	-1.600040×10^7	2.338152×10^7	-1.518654×10^7	3.699165×10^6
5	3.772163×10^4	-1.459921×10^5	2.118728×10^5	-1.366459×10^5	3.304777×10^4

Table A3. The coefficient matrix $Q_{E_{(0.1-0.96)}}$.

$Q_E(i,j)$	1	2	3	4	5	6	7	8
1	-1.214129×10^5	4.080502×10^5	-5.578232×10^5	3.992182×10^5	-1.594275×10^5	3.540716×10^4	-3.893465×10^3	-1.118158×10^2
2	8.136427×10^4	-2.751853×10^5	3.777982×10^5	-2.713634×10^5	1.086416×10^5	-2.420097×10^4	2.694569×10^3	1.743043×10^2
3	-1.445757×10^4	4.954249×10^4	-6.859222×10^4	4.961920×10^4	-1.995944×10^4	4.469279×10^3	-5.215943×10^2	-9.239491×10^1
4	1.238708×10^3	-4.258676×10^3	5.912241×10^3	-4.284829×10^3	1.728524×10^3	-3.841652×10^2	5.221578×10^1	1.873416×10^1
5	6.145656×10^1	-2.492580×10^2	4.310867×10^2	-4.105013×10^2	-3.873198	-2.873198	-1.873198	-8.731984×10^{-1}

References

1. Moore, R.B.; Raman, V. Hydrogen infrastructure for fuel cell transportation. *Int. J. Hydrogen Energy* **1998**, *23*, 617–620. [CrossRef]
2. Berberoğlu, H.; Yin, J.; Pilon, L. Light transfer in bubble sparged photobioreactors for H_2 production and CO_2 mitigation. *Int. J. Hydrogen Energy* **2007**, *32*, 2273–2285. [CrossRef]
3. Fang, H.H.; Liu, H.; Zhang, T. Phototrophic hydrogen production from acetate and butyrate in wastewater. *Int. J. Hydrogen Energy* **2005**, *30*, 785–793. [CrossRef]
4. Das, D.; Veziroğlu, T.N. Hydrogen production by biological processes: A survey of literature. *Int. J. Hydrogen Energy* **2001**, *26*, 13–28. [CrossRef]
5. Ghirardi, M.L.; Alexandra, D.; Yu, J.P. Photobiological hydrogen-producing systems. *Chem. Soc.* **2008**, *38*, 52–61. [CrossRef]
6. Melis, A.; Zhang, L.; Forestier, M.; Ghirardi, M.L.; Seibert, M. Sustained photobiological hydrogen gas production upon reversible inactivation of oxygen evolution in the green alga *Chlamydomonas reinhardtii*. *Plant Physiol.* **2000**, *112*, 127–135. [CrossRef]
7. Melis, A. Green alga hydrogen production: Progress, challenges and prospects. *Int. J. Hydrogen Energy* **2002**, *27*, 1217–1228. [CrossRef]
8. Berberoğlu, H.; Gomez, P.S.; Pilon, L. Radiation characteristics of Botryococcus braunii, Chlorococcum littorale, and Chlorella sp. used for CO_2 fixation and biofuel production. *J. Quant. Spectrosc. Radiat. Transf.* **2009**, *110*, 1879–1893. [CrossRef]
9. He, Z.Z.; Qi, H.; He, M.J.; Ruan, L.M. Experimental research on the photobiological hydrogen production kinetic of Chlamydomonas reinhardtii GY-D55. *Int. J. Hydrogen Energy* **2016**, *41*, 15651–15660. [CrossRef]
10. Berberoğlu, H.; Pilon, L. Experimental measurements of the radiation characteristics of Anabaena variabilis ATCC 29413-U and Rhodobacter sphaeroides ATCC 49419. *Int. J. Hydrogen Energy* **2007**, *32*, 4772–4785. [CrossRef]
11. Aiba, S. *Growth Kinetics of Photosynthetic Microorganisms*; Springer: Berlin, Germany, 1982; pp. 85–156.
12. Berberoğlu, H.; Pilon, L. Maximizing the solar to H_2 energy conversion efficiency of outdoor photobioreactors using mixed cultures. *Int. J. Hydrogen Energy* **2010**, *35*, 500–510. [CrossRef]
13. Murphy, T.E.; Berberoğlu, H. Effect of algae pigmentation on photobioreactor productivity and scale-up: A light transfer perspective. *J. Quant. Spectrosc. Radiat. Transf.* **2011**, *112*, 2826–2834. [CrossRef]
14. Wheaton, Z.C.; Krishnamoorthy, G. Modeling radiative transfer in photobioreactors for algal growth. *Comput. Electron. Agric.* **2012**, *87*, 64–73. [CrossRef]
15. Slegers, P.; Wijffels, R.; Van Straten, G.; Van Boxtel, A. Design scenarios for flat panel photobioreactors. *Appl. Energy* **2011**, *88*, 3342–3353. [CrossRef]
16. Pruvost, J.; Cornet, J.; Goetz, V.; Legrand, J. Theoretical investigation of biomass productivities achievable in solar rectangular photobioreactors for the cyanobacterium arthrospira platensis. *Biotechnol. Progr.* **2012**, *28*, 699–714. [CrossRef]
17. Lee, E.; Pruvost, J.; He, X.; Munipalli, R.; Pilon, L. Design tool and guidelines for outdoor photobioreactors. *Chem. Eng. Sci.* **2014**, *106*, 18–29. [CrossRef]
18. Zhang, J.Y.; Qi, H.; He, Z.Z.; Yu, X.Y.; Ruan, L.M. Investigation of light transfer procedure and photobiological hydrogen production of microalgae in photobioreactors at different location of China. *Int. J. Hydrogen Energy* **2017**, *42*, 19709–19722. [CrossRef]
19. Laurinavichene, T.; Tolstygina, I.; Tsygankov, A. The effect of light intensity on hydrogen production by sulfur-deprived *Chlamydomonas reinhardtii*. *J. Biotechnol.* **2004**, *114*, 143–151. [CrossRef]
20. Hale, G.M.; Querry, M.R. Optical constants of water in the 200-nm to 200-µm wavelength region. *Appl. Opt.* **1973**, *12*, 555–563. [CrossRef]
21. Lee, E.; Heng, R.L.; Pilon, L. Spectral optical properties of selected photosynthetic microalgae producing biofuels. *J. Quant. Spectrosc. Radiat. Transf.* **2013**, *114*, 122–135. [CrossRef]
22. Modest, M.F. *Radiative Heat Transfer*, 3rd ed.; McGraw-Hill: New York, NY, USA, 2013; pp. 362–371.
23. Pilon, L.; Berberoğlu, H.; Kandilian, R. Radiation transfer in photobiological carbon dioxide fixation and fuel production by microalgae. *J. Quant. Spectrosc. Radiat. Transf.* **2011**, *112*, 2639–2660. [CrossRef]

24. Dunn, I.J.; Heinzle, E.; Ingham, J.; Ji, E.P. *Biological Reaction Engineering: Dynamic Modelling Fundamentals with Simulation Examples*; Wiley-VCH: Weinheim, Germany, 2013; pp. 254–268.
25. He, Z.Z.; Qi, H.; Chen, Q.; Ruan, L.M. Retrieval of aerosol size distribution using improved quantum-behaved particle swarm optimization on spectral extinction measurements. *Particuology* **2014**, *28*, 6–14. [CrossRef]